Identification of an IFN-γ/mast cell axis in a mouse model of chronic asthma

Mang Yu,[1] Michael R. Eckart,[2] Alexander A. Morgan,[3] Kaori Mukai,[1] Atul J. Butte,[3] Mindy Tsai,[1] and Stephen J. Galli[1,4]

[1]Department of Pathology, [2]Department of Protein and Nucleic Acid Biotechnology Facility, [3]Department of Pediatrics and Center for Pediatric Bioinformatics, and [4]Department of Microbiology and Immunology, Stanford University School of Medicine, Stanford, California, USA.

Asthma is considered a Th2 cell–associated disorder. Despite this, both the Th1 cell–associated cytokine IFN-γ and airway neutrophilia have been implicated in severe asthma. To investigate the relative contributions of different immune system components to the pathogenesis of asthma, we previously developed a model that exhibits several features of severe asthma in humans, including airway neutrophilia and increased lung IFN-γ. In the present studies, we tested the hypothesis that IFN-γ regulates mast cell function in our model of chronic asthma. Engraftment of mast cell–deficient $Kit^{W-sh/W-sh}$ mice, which develop markedly attenuated features of disease, with wild-type mast cells restored disease pathology in this model of chronic asthma. However, disease pathology was not fully restored by engraftment with either IFN-γ receptor 1–null ($Ifngr1^{-/-}$) or Fcε receptor 1γ–null ($Fcer1g^{-/-}$) mast cells. Additional analysis, including gene array studies, showed that mast cell expression of IFN-γR contributed to the development of many FcεRIγ-dependent and some FcεRIγ-independent features of disease in our model, including airway hyperresponsiveness, neutrophilic and eosinophilic inflammation, airway remodeling, and lung expression of several cytokines, chemokines, and markers of an alternatively activated macrophage response. These findings identify a previously unsuspected IFN-γ/mast cell axis in the pathology of chronic allergic inflammation of the airways in mice.

Introduction

Asthma is a complex disorder characterized by chronic inflammation of the airways, airway hyperresponsiveness (AHR), airflow obstruction, and airway wall remodeling (1, 2). Many features of asthma are thought to reflect consequences of Th2-dominated immune responses to allergens in which Th2-type cytokines such as IL-4 and IL-13, and the Th2-associated immunoglobulin IgE, contribute to intricate pathways that result in inflammation and tissue damage (3). Mast cells are considered critical for the development of asthma phenotypes because of their ability to release, upon activation by IgE and specific antigen, a diverse range of autacoid mediators, chemokines, cytokines, and growth factors (4). Infiltration of the airway with eosinophils is also thought to be important in the pathology of asthma (1–4).

However, studies of patients with well-characterized asthma have suggested that neutrophils, in addition to eosinophils, may have important roles in asthma (5). Patients with chronic severe or acute fatal asthma exhibit increased numbers of airway neutrophils (6–9), and neutrophilic inflammation is positively correlated with the severity of airflow obstruction (10, 11). Moreover, airway neutrophilia and eosinophilia are not mutually exclusive (10, 12). Patients with severe asthma, compared with those with mild or moderate asthma, have both a greater percentage of sputum neutrophils and evidence for higher continuing release of eosinophil-derived mediators (13).

Other evidence suggests a possible role for the Th1 cell–associated cytokine INF-γ, as well as Th2 cell–associated cytokines, in some asthmatic subjects. Leukocytes in the BAL fluid from asthma patients can produce IFN-γ ex vivo (14), and, compared with moderate asthmatics, patients with severe asthma exhibit increased

numbers of sputum neutrophils and eosinophils, increased epithelial or subepithelial expression of IFN-γ or IL-8, and decreased subepithelial expression of IL-4 (15). Increased lung levels of IFN-γ (16) or other evidence for the involvement of this cytokine (17–23) have been reported in some mouse models of allergic inflammation of the airways, but such studies have indicated that Th1 responses (17–19, 23) or IFN-γ (20–22) may have effects that counteract (18–20), enhance (17, 21, 23), or prolong (22) features of Th2 responses in these settings.

While the different results in various studies regarding the potential roles of IFN-γ in allergic airway inflammation may reflect, at least in part, differences in the mouse models and/or experimental approaches that were employed, taken together this prior work indicates that Th2- and Th1-associated pathways can interact in such settings (16, 17, 23, 24). There are many potential sources of IFN-γ during airway inflammation, including activated CD4+ Th1 cells, CD8+ T cells, and NK cells, as well as γδT cells, macrophages, dendritic cells, NKT cells, naive CD4+ T cells, and B cells (25–27). Whatever its cellular source, IFN-γ can exert pleiotropic effects through a receptor complex (IFN-γ receptor [IFN-γR]) composed of two chains: IFN-γR1 (also known as IFN-γRα), the major ligand-binding subunit, and IFN-γR2 (also known as IFN-γRβ), which is required for IFN-γ signal transduction and for increasing the affinity of IFN-γR1 to its ligand (25, 28).

We developed a mouse model of chronic allergic inflammation of the airways that exhibits several features of chronic asthma in humans, including inflammatory responses in the lungs that include both neutrophils and eosinophils (29). Most features of this model were markedly attenuated or absent in genetically mast cell–deficient mice, and optimal development of many of these "mast cell–dependent" characteristics required mast cell expression of Fcε receptor 1γ (FcεRIγ), which is necessary for mast cell activation via FcεRI-bound IgE and specific antigen or by immune
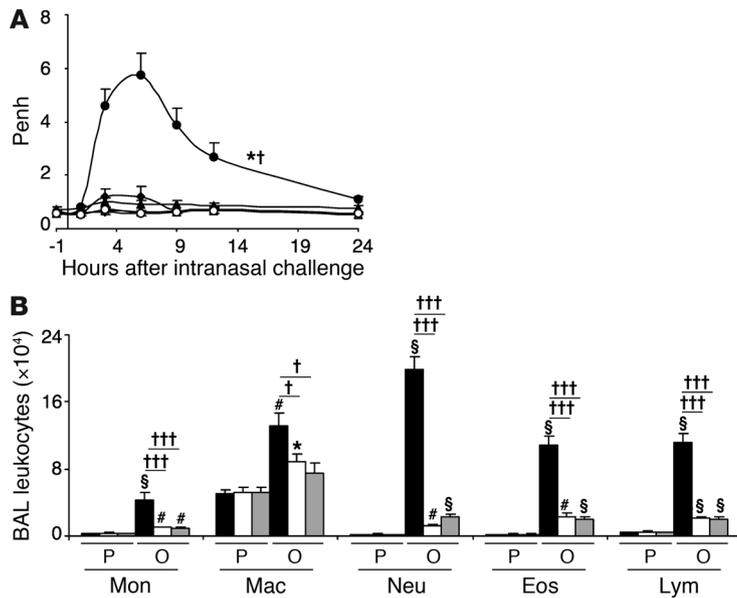
Figure 1
Influence of IFN-γ or IFN-γR1 on the development of airway responses and leukocytes in BAL fluid. (**A**) Airway responses (assessed as Penh) measured in OVA-sensitized and -challenged WT C57BL/6 (filled circles), *Ifng*$^{-/-}$ (filled triangles), and *Ifngr1*$^{-/-}$ (filled diamonds) mice, and in PBS-treated C57BL/6 (open circles), *Ifng*$^{-/-}$ (open triangles), and *Ifngr1*$^{-/-}$ (open diamonds) mice at 1 hour before and 1, 3, 6, 9, 12, and 24 hours after the ninth OVA or PBS challenge; n = 6–12 per group. (**B**) Numbers of leukocytes in BAL fluid from the right lung of C57BL/6 (black bars), *Ifng*$^{-/-}$ (white bars), or *Ifngr1*$^{-/-}$ (gray bars) mice following OVA sensitization and challenge (O) or PBS treatment (P). *$P < 0.05$, #$P < 0.01$, §$P < 0.001$ versus corresponding PBS-treated controls; †$P < 0.05$, †††$P < 0.001$ versus each of the other groups (in **A**) or versus the groups indicated (n = 6–12 per group). Mon, monocytes; Mac, macrophages; Neu, neutrophils; Eos, eosinophils; Lym, lymphocytes.

complexes of IgG$_1$ bound to FcγRIII (29). We found that mice subjected to this model developed greatly increased lung expression of a T cell–specific GTPase selectively induced by IFN-γ (29, 30).

Receptors for IFN-γ have been detected on mouse (31) and human (32) mast cells, and stimulation of various mast cell populations with IFN-γ in vitro has been reported to increase histamine release in anti-IgE–stimulated in vitro derived human mast cells (32), decrease serotonin release in mouse peritoneal mast cells stimulated with IgE plus antigen (IgE+Ag) (33) and decrease histamine release in antigen-stimulated rat peritoneal mast cells (34), and have no significant effect on antigen-stimulated histamine release in rat intestinal mast cells (34). While these in vitro studies suggest that the effects of INF-γ on mast cell activation may vary according to species and/or anatomic site, the importance of INF-γ in regulating mast cell function in vivo has not been investigated. However, given the evidence that INF-γ can influence mast cell function in vitro, we were intrigued by the idea that IFN-γ might regulate mast cell function in our model of chronic allergic inflammation of the airways.

In the present study, we tested this hypothesis by evaluating the effects of IFN-γ on mast cell function in vitro and by comparing features of our chronic asthma model in WT, *Ifng*$^{-/-}$, and *Ifngr1*$^{-/-}$ mice and in genetically mast cell–deficient *Kit*$^{W-sh/W-sh}$ mice engrafted with WT, *Ifngr1*$^{-/-}$, or *Fcer1g*$^{-/-}$ mast cells.

Results

IFN-γ and IFN-γR contribute to this model of chronic allergic inflammation. We first evaluated whether IFN-γ or IFN-γR contributes to airway responsiveness to antigen or airway inflammation in this model (29). As expected (29), WT mice exhibited a significant increase in enhanced pause (Penh, a measure of airway resistance in unrestrained, non-anesthetized mice) after antigen challenge, with the peak of responsiveness occurring between 3 and 9 hours after OVA challenge, whereas *Ifng*$^{-/-}$ or *Ifngr1*$^{-/-}$ mice exhibited significantly attenuated Penh responses to OVA challenge (Figure 1A). OVA-sensitized *Ifng*$^{-/-}$ and *Ifngr1*$^{-/-}$ mice also exhibited significantly decreased numbers of total BAL fluid leukocytes after

OVA challenge, as well as significant reductions in individual types of leukocytes, including monocytes, macrophages, neutrophils, eosinophils, and lymphocytes (Figure 1B). We also found that, in WT C57BL/6 mice, i.p. treatment with a single dose of 5 μg IFN-γ, given 30 minutes before or 3 hours after the last of 9 intranasal (i.n.) challenges with OVA, significantly increased both the Penh response to that OVA challenge and the number of neutrophils in the BAL fluid 24 hours after OVA challenge (Supplemental Figure 1; supplemental material available online with this article; doi:10.1172/JCI43598DS1). By contrast, treatment with a neutralizing antibody to IFN-γ (100 μg per mouse, i.p., at 3 hours after the ninth OVA challenge), compared with treatment with an isotype-matched control antibody, significantly reduced both the Penh response to that OVA challenge and the number of neutrophils, eosinophils, and lymphocytes in the BAL fluid 24 hours after OVA challenge (Supplemental Figure 1). Taken together, these results support the conclusion that IFN-γ and the IFN-γR can significantly enhance these features of the model, but do not clarify which IFN-γR–bearing cell type(s) contributed to these effects.

IFN-γ can increase mast cell production of histamine and cytokines in vitro. Because many features of this model require mast cells and mast cell expression of the FcεRIγ chain for full development (29), we next evaluated whether IFN-γ can influence mast cell activation via FcεRI. Bone marrow–derived cultured mast cells (BMCMCs) generated in vitro from WT, IFN-γR1–deficient, or FcεRIγ-deficient mice were sensitized overnight with an anti-dinitrophenol–specific (anti-DNP–specific) monoclonal mouse IgE and then challenged for 1 hour or 24 hours with various concentrations of specific antigen (DNP-HSA) with or without IFN-γ at 1 or 5 ng/ml. Activation of mast cells with IgE+Ag resulted in the dose-dependent secretion of histamine, IL-6, and IL-13 by WT or *Ifngr1*$^{-/-}$ BMCMCs (Figure 2), but no detectable release of IL-4, IFN-γ, or the chemokines CXCL1, CXCL2, CCL9, CCL11, CCL12, or CCL24. IFN-γ significantly increased the release of histamine, IL-6, and IL-13 by IgE+Ag-stimulated WT BMCMCs, whereas treatment of the cells with IFN-γ alone was without effect (Figure 2 and Supplemental Figure 2). FcεRIγ-deficient BMCMCs were not detectably respon-
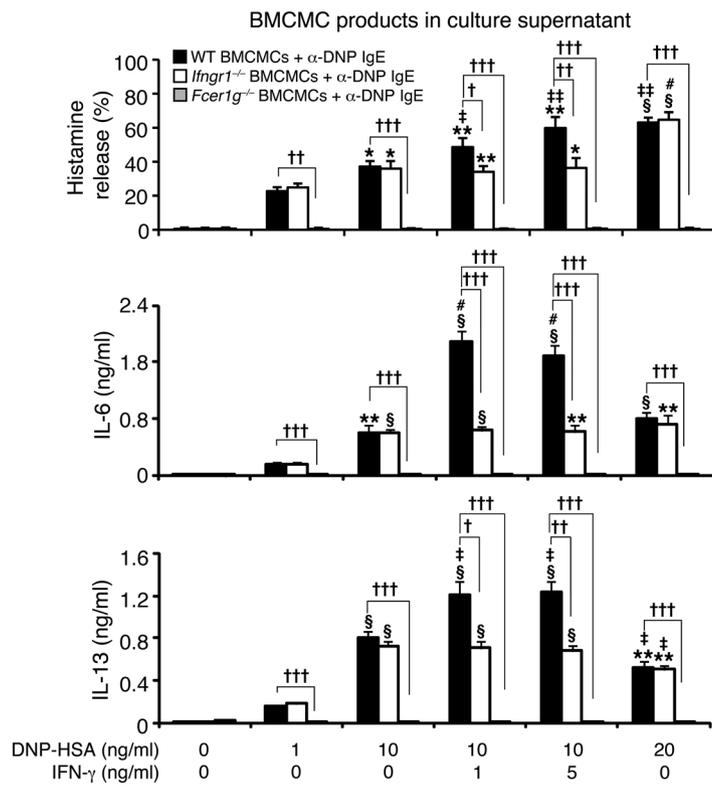
Figure 2
Influence of IFN-γ on the expression of mast cell function in vitro. Culture supernatants of anti-DNP IgE-sensitized BMCMCs from WT C57BL/6 (black bars), *Ifngr1*^{−/−} (white bars), or *Fcer1g*^{−/−} (gray bars) mice were collected 1 hour (for calculation of % histamine release) or 24 hours (for measurement of secreted cytokines) after addition of DNP-HSA or DNP/IFN-γ. Data were calculated from results pooled from 3 independent experiments, each of which gave similar results. IL-6 levels in supernatants collected from the cultures of WT BMCMCs stimulated with 1 or 5 ng/ml of IFN-γ in the absence of DNP-HSA were 0.009 ± 0.002 or 0.007 ± 0.002 ng/ml; the corresponding IL-13 levels were 0.015 ± 0.003 or 0.018 ± 0.004 ng/ml, respectively. *P < 0.05, **P < 0.01, §P < 0.001 versus values from the corresponding BMCMCs stimulated with 1 ng/ml DNP-HSA alone. †P < 0.05, ††P < 0.01, †††P < 0.001 versus group indicated. ‡P < 0.05, ‡‡P < 0.01, #P < 0.001 versus values from the corresponding BMCMCs stimulated with 10 ng/ml DNP-HSA alone. n = 3 per group.

sive to IgE+Ag challenge, with or without IFN-γ (Figure 2). The ability of IFN-γ to enhance dose-dependently the IgE+Ag-induced mast cell production of IL-13 is of particular interest (Supplemental Figure 2), since IL-13 is thought to contribute to the development of asthma through such effects as promoting subepithelial fibrosis (in part by upregulating synthesis of arginase-1), increasing mucus secretion, and eliciting AHR (35).

Lung expression of IFN-γ. To assess the importance of mast cell signaling via IFN-γR versus FcεRIγ in vivo, we compared features of our model in 5 groups of age-matched mice, all of them on the C57BL/6 background: WT mice, genetically mast cell–deficient *Kit*[W-sh/W-sh] mice, and *Kit*[W-sh/W-sh] mice engrafted with mast cells derived from WT, IFN-γR1–deficient, or FcεRIγ–deficient mice. Compared with PBS treatment in control groups, OVA sensitization and challenge resulted in significant increases in the amounts of IFN-γ in the lungs of each of the 5 types of mice tested (including the profoundly mast cell–deficient *Kit*[W-sh/W-sh] mice) (Figure 3A). By contrast, none of the groups of OVA-sensitized mice exhibited levels of lung IL-4 after OVA challenge that differed significantly

from those in the corresponding PBS-treated groups (Figure 3B). OVA-sensitized and -challenged mice also exhibited elevations in lung levels of IL-17, a cytokine that has been implicated in the development of neutrophilic infiltrates in several settings (36); however, all groups of OVA-challenged mice developed similar elevations in lung levels of IL-17 (Supplemental Figure 3).

Mast cell IFN-γR can increase airway responses to antigen or methacholine. OVA-treated WT mice or *Kit*[W-sh/W-sh] mice engrafted with WT mast cells (WT BMCMCs→*Kit*[W-sh/W-sh] mice) exhibited significantly increased Penh responses to methacholine (a measure of AHR) or to antigen, while little or no enhancement of Penh responses to methacholine or antigen occurred in identically sensitized and challenged mast cell–deficient *Kit*[W-sh/W-sh] mice or in *Kit*[W-sh/W-sh] mice engrafted with *Ifngr1*^{−/−} or *Fcer1g*^{−/−} mast cells (*Ifngr1*^{−/−} BMC-MCs→*Kit*[W-sh/W-sh] or *Fcer1g*^{−/−} BMCMCs→*Kit*[W-sh/W-sh] mice) (Figure 4, A and B, and Supplemental Figure 4, A and B). Similar results were obtained when we measured the effects of methacholine challenge on lung resistance (R_L) and dynamic compliance (C_{dyn}) in anesthetized, tracheostomized mice (Figure 4, C and D, and
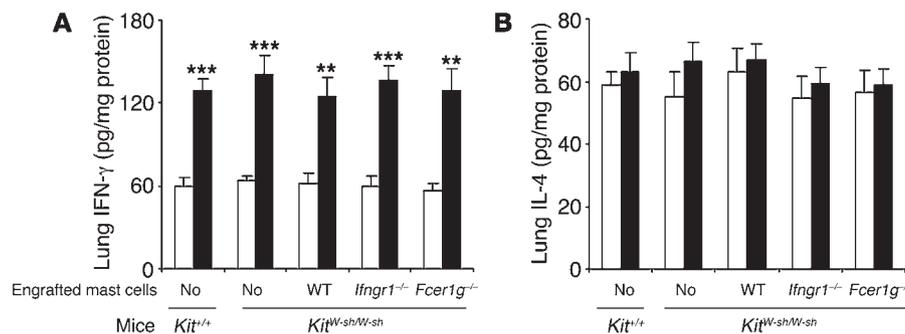
Figure 3
Lung expression of IFN-γ and IL-4. (**A** and **B**) Tissues were sampled 24 hours after the 9th OVA or PBS challenge. White bars, PBS-treated groups; black bars, OVA-sensitized and -challenged groups. **P < 0.01, ***P < 0.001 versus the corresponding PBS controls; n = 6–10 per group.
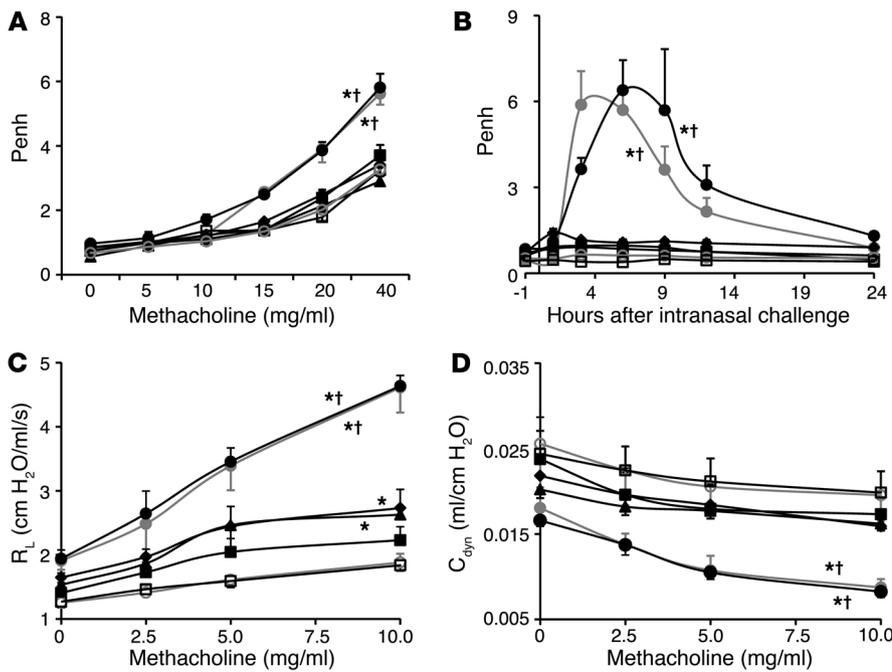
Figure 4
Airway responses following i.n. challenge with antigen (OVA) or PBS. (**A**) Penh responses to aerosolized methacholine measured 24 hours after the eighth OVA or PBS challenge. (**B**) OVA or PBS challenge–induced changes in Penh measured 1 hour before and 1, 3, 6, 9, 12, and 24 hours after the ninth OVA or PBS challenge. (**C** and **D**) Changes in R_L and C_{dyn} to aerosolized methacholine administered 24 hours after the ninth OVA or PBS challenge. Data are from OVA-sensitized and challenged WT C57BL/6 (filled gray circles), mast cell–deficient C57BL/6-$Kit^{W-sh/W-sh}$ (filled black squares), C57BL/6 BMCMCs→ C57BL/6-$Kit^{W-sh/W-sh}$ (filled black circles), $Ifngr1^{-/-}$ BMCMCs→ C57BL/6-$Kit^{W-sh/W-sh}$ (filled black diamonds), and $Fcer1g^{-/-}$ BMCMCs→ C57BL/6-$Kit^{W-sh/W-sh}$ (filled black triangles) mice and the corresponding PBS-treated control mice (open gray circles or open squares [shown here and in Supplemental Figure 4, representing control data for WT C57BL/6 and mast cell–deficient C57BL/6-$Kit^{W-sh/W-sh}$ mice]). See Supplemental Figure 4 for the control data for the different groups of mast cell–engrafted C57BL/6-$Kit^{W-sh/W-sh}$ mice. *$P < 0.05$ versus the corresponding PBS controls; †$P < 0.05$ versus each of the other groups except the OVA-sensitized and challenged C57BL/6 or C57BL/6 BMCMCs→ C57BL/6-$Kit^{W-sh/W-sh}$ group. $n = 6$–12 per group (**A** and **B**); $n = 4$–6 per group (**C** and **D**).

Supplemental Figure 4, C and D). Compared with responses in PBS-treated mice, only OVA-sensitized WT mice and WT BMC-MCs→$Kit^{W-sh/W-sh}$ mice exhibited significant reductions in C_{dyn} in response to methacholine challenge (Figure 4D and Supplemental Figure 4D). We detected slightly but significantly increased R_L following methacholine challenge in OVA-sensitized and -challenged $Ifngr1^{-/-}$ BMCMCs→$Kit^{W-sh/W-sh}$ and $Fcer1g^{-/-}$ BMCMCs→$Kit^{W-sh/W-sh}$ mice, but these responses were significantly less intense than those in the corresponding WT mice and WT BMCMCs→$Kit^{W-sh/W-sh}$ mice (Figure 4C and Supplemental Figure 4C). These findings indicate that the development of airway responses to antigen and airway hyperreactivity to cholinergic stimulation in this model is largely dependent on mast cell IFN-γR, as well as mast cell FcεRIγ. All 5 groups of OVA-sensitized mice exhibited similar elevations in plasma levels of OVA-specific IgE and IgG₁ antibodies (Supplemental Figure 5).

Taken together, our findings indicate that the development of airway reactivity to antigen and airway hyperreactivity to cholinergic stimulation in this model is largely dependent on mast cell IFN-γR, as well as mast cell FcεRIγ. Our data also suggest that the

critical mast cell–dependent effects in this model primarily are those that influence end-organ tissue manifestations of antigen challenge in sensitized mice, rather than any potential mast cell–dependent effects on sensitization to antigen and/or the generation of antigen-specific IgE or IgG₁ antibodies.

Mast cell IFN-γR can increase airway inflammation. Histologic analysis (Figure 5, A–E, K, and L) and examination of BAL fluids (Figure 5N) confirmed that mast cells are required for optimal development of antigen-induced lung inflammation in this model (29) and showed, unexpectedly, that such leukocyte infiltration was markedly and significantly reduced in mice in which only mast cells lacked IFN-γR, as well as in those in which only mast cells lacked FcεRIγ. Baseline numbers of mast cells/ mm² of peribronchial tissue were similar in all groups of PBS-treated control mice except $Kit^{W-sh/W-sh}$ mice, which totally lacked mast cells (Figure 5, F–J and M). We did not detect differences in the anatomical distribution of the 3 different types of mast cells (i.e., WT, $Ifngr1^{-/-}$, and $Fcer1g^{-/-}$) that had been adoptively transferred into the $Kit^{W-sh/W-sh}$ mice, either in PBS-treated or OVA sensitized and challenged mice. However, as has been reported for mast cell–engrafted WBB6F₁-$Kit^{W/W-v}$ (37) and C57BL/6-$Kit^{W-sh/W-sh}$ (38, 39) mice, $Kit^{W-sh/W-sh}$ mice containing adoptively transferred mast cells exhibited more mast cells in the periphery of the lungs than did WT mice. OVA treatment significantly increased the number of peribronchial mast cells in WT BMCMCs→$Kit^{W-sh/W-sh}$ and $Ifngr1^{-/-}$ BMC-MCs→$Kit^{W-sh/W-sh}$ mice, but not in $Fcer1g^{-/-}$ BMCMCs→$Kit^{W-sh/W-sh}$ mice (Figure 5, F–J and M). These findings confirmed that mast cells must express FcεRIγ in order to undergo significant expansion in this model (29) and show that this antigen-induced increase in mast cell numbers does not require that the mast cell be able to respond to IFN-γ via IFN-γR.

Mast cell IFN-γR can increase airway remodeling. We confirmed that mast cells are required for the full development of features of antigen-induced airway remodeling in this model (29), including subepithelial fibrosis (Figure 6, A–C), increases in lung collagen (Figure 6F), and hyperplasia of mucus-secreting goblet cells (Figure 6G), and that mast cell expression of FcεRIγ contributed more substantially to the development of increased lung collagen than to goblet cell hyperplasia in this model (Figure 6, F and G, and ref. 29). Moreover, mice in which only mast cells lacked IFN-γR exhibited impairment in the antigen-induced development of increased levels of subepithelial fibrosis (Figure 6, A–E), lung collagen (Figure 6F), and airway goblet cells (Figure 6G) that were very similar to those observed in mice in which only mast cells lacked FcεRIγ.

Mast cell expression of each receptor also was required for optimal antigen-induced and mast cell–dependent increases in lung lev-
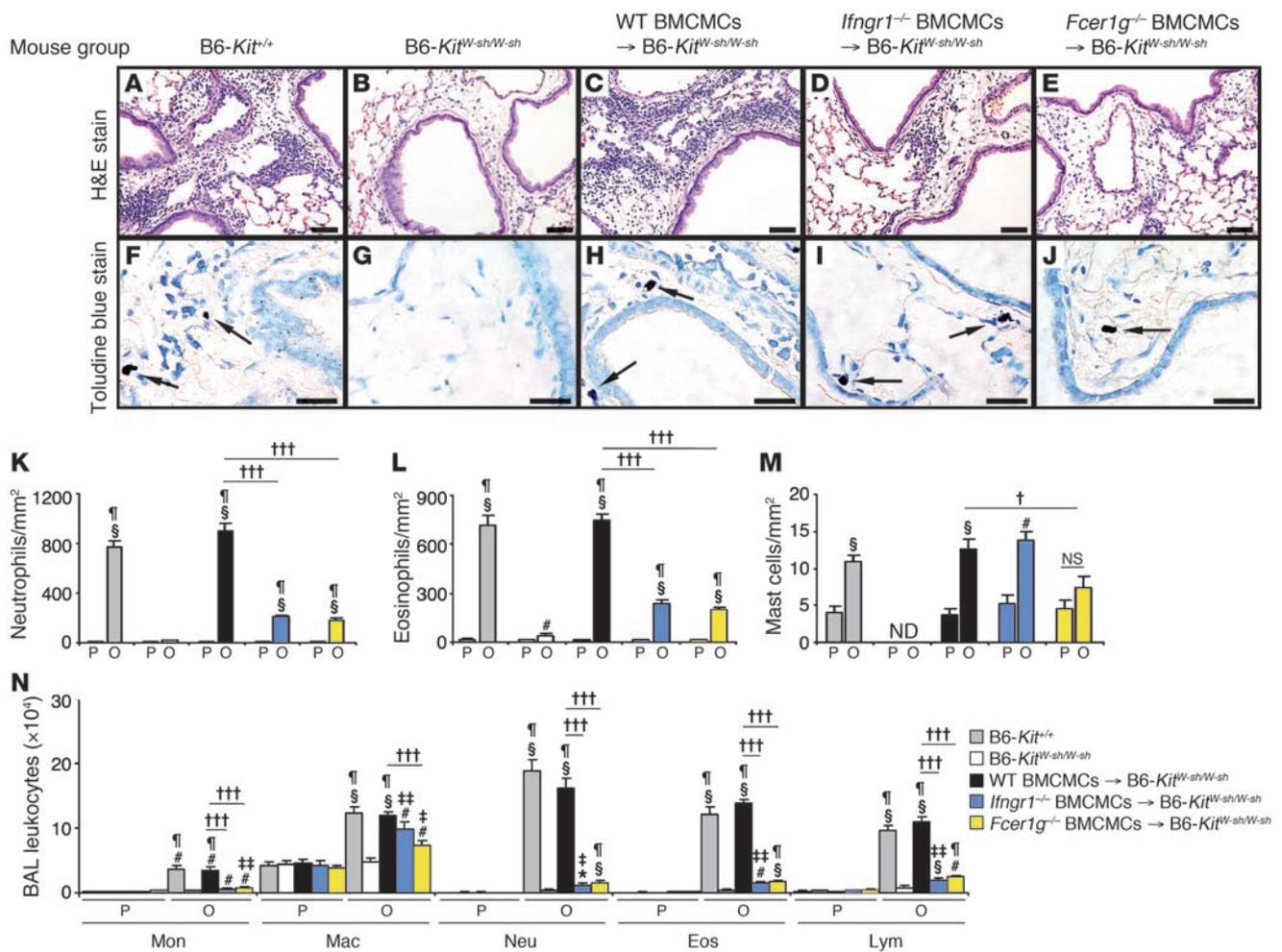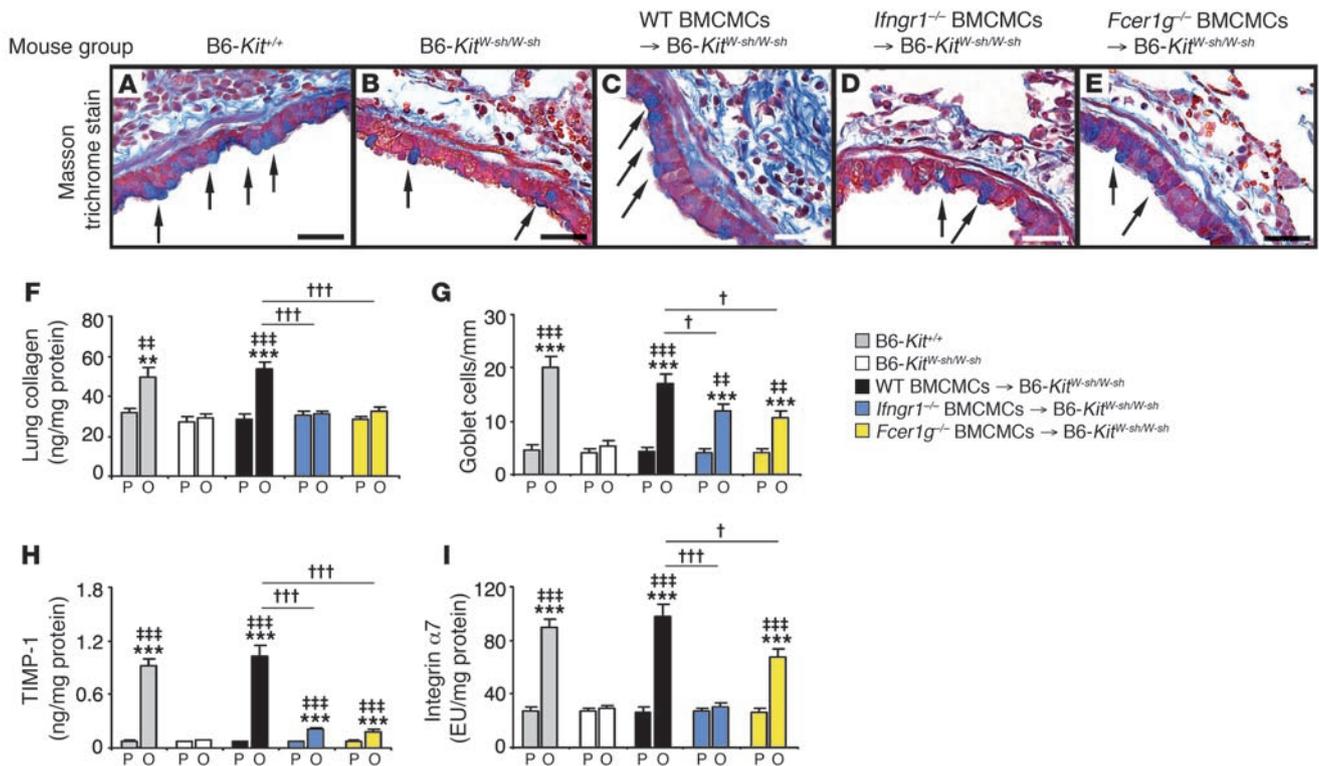
Figure 5
Features of lung inflammation. H&E-stained (**A–E**) and toluidine blue–stained (**F–J**) tissue sections demonstrating peribronchial inflammatory infiltrates and mast cells (indicated with arrows) in the lungs 24 hours after the ninth OVA challenge; (**K–M**) numbers of various cell types in the lungs; (**N**) numbers of leukocytes in BAL fluid recovered from the right lungs 24 hours after the ninth OVA or PBS challenge. B6, C57BL/6. Data are from WT C57BL/6 (gray bars), mast cell–deficient C57BL/6-*Kit^W-sh/W-sh* (white bars), C57BL/6 BMCMCs→ C57BL/6-*Kit^W-sh/W-sh* (black bars), *Ifngr1^−/−* BMCMCs→ C57BL/6-*Kit^W-sh/W-sh* (blue bars), and *Fcer1g^−/−* BMCMCs→ C57BL/6-*Kit^W-sh/W-sh* (yellow bars) mice and the corresponding PBS-treated control mice. *$P < 0.05$, #$P < 0.01$, §$P < 0.001$ versus the corresponding PBS controls; ‡$P < 0.05$, ‡‡$P < 0.01$, ¶$P < 0.001$ versus OVA-sensitized and -challenged *Kit^W-sh/W-sh* mice; †$P < 0.05$, †††$P < 0.001$ versus group indicated. ND, not detected. $n = 6$ to 12 per group. Scale bars: 50 μm.

els of tissue inhibitor of metalloproteinases–1 (TIMP-1) and integrin α7 (Figure 6, H and I). TIMP-1, a major inhibitor of MMP-9, is thought to contribute to a profibrotic environment and airway remodeling by reducing extracellular matrix turnover (40). Integrin α7 is thought to regulate smooth muscle cell proliferation and is required for the expression of a contractile phenotype by human airway myocytes (41, 42). In mice in which mast cells lacked either FcεRIγ or IFN-γR, we observed only minimal (albeit statistically significant) antigen-induced increases in TIMP-1 (Figure 6H). By contrast, the development of antigen-dependent increases in lung levels of integrin α7 appeared to be virtually entirely dependent on mast cell expression of INF-γR, whereas this effect was still evident, although at a significantly (~32%) reduced level, in mice whose mast cells lacked FcεRIγ (Figure 6I).

Mast cell IFN-γR is required for optimal expression of lung chemokines. C-X-C chemokines, including CXCL1 and CXCL2, are predomi-

nantly chemotactic for neutrophils, whereas chemokines with C-C motifs are predominantly chemotactic for monocytes, macrophages, dendritic cells, lymphocytes, NK cells, eosinophils, and basophils (43). Using a microarray-based analysis of lung gene expression as a screening tool (GEO GSE27066), we found that OVA sensitization and challenge induced markedly increased lung levels of mRNA for CXCL1, CXCL2, CCL11, CCL12, and CCL24 in WT mice and in WT BMCMCs→*Kit^W-sh/W-sh* mice, but not in mast cell–deficient *Kit^W-sh/W-sh* mice; we then confirmed these findings by measuring lung levels of the corresponding proteins (Supplemental Figure 6). Levels of these chemokines in OVA-treated mice whose mast cells lacked either IFN-γR or FcεRIγ were very similar to those in mast cell–deficient *Kit^W-sh/W-sh* mice (there was a minimal, but statistically significant, OVA-induced increase in levels of lung CXCL1 in *Ifngr1^−/−* BMCMCs→*Kit^W-sh/W-sh* mice) (Supplemental Figure 6A). OVA treatment induced an increase in lung CCL9 levels

Figure 6
Features of airway wall remodeling. (**A–E**) Masson's trichrome–stained tissue sections demonstrating mucus-secreting goblet cells (blue, indicated with arrows) and subepithelial fibrosis (collagen stains blue). (**F–I**) Collagen levels in the lung (**F**), numbers of goblet cells along the airway epithelium (**G**), and levels of lung TIMP-1 (**H**) and integrin $\alpha 7$ (**I**). Data are from WT C57BL/6 (gray bars), mast cell–deficient C57BL/6-$Kit^{W-sh/W-sh}$ (white bars), C57BL/6 BMCMCs→ C57BL/6-$Kit^{W-sh/W-sh}$ (black bars), $Ifngr1^{-/-}$ BMCMCs→ C57BL/6-$Kit^{W-sh/W-sh}$ (blue bars), and $Fcer1g^{-/-}$ BMC-MCs→ C57BL/6-$Kit^{W-sh/W-sh}$ (yellow bars) mice and the corresponding PBS-treated control mice. ******$P < 0.01$, *******$P < 0.001$ versus the corresponding PBS controls; ‡‡$P < 0.01$, ‡‡‡$P < 0.001$ versus OVA-sensitized and -challenged $Kit^{W-sh/W-sh}$ mice; †$P < 0.05$, †††$P < 0.001$ versus group indicated. $n = 6$–10 per group in **F–I**. Scale bars (in **A–E**): 30 μm. EU, experimental units, with the arbitrary value of 100 EU assigned to the mean value for the integrin $\alpha 7$ content in the lung protein extract of 4 randomly selected WT C57BL/6 mice in the OVA-sensitized and -challenged group.

that was largely, but not entirely, mast cell dependent, and the mast cell–dependent increase in levels of CCL9 in antigen-treated mice required mast cell expression of both IFN-γR and FcεRIγ (Supplemental Figure 6C).

These findings show that mast cells greatly increase lung levels of several chemokines in this model, including those that are chemotactic for neutrophils, eosinophils, monocytes, and lymphocytes, cells whose numbers in the lungs are regulated in a largely mast cell–dependent manner (Figure 5, A–C, K, L, and N). Moreover, mast cell transfer studies indicated that the ability of mast cells to enhance lung levels of these chemokines in $Kit^{W-sh/W-sh}$ mice was virtually ablated if the adoptively transferred mast cells lacked either IFN-γR or FcεRIγ (Supplemental Figure 6). By contrast, antigen-dependent changes in lung levels of IL-17 occurred independently of mast cells (Supplemental Figure 3).

Inflammatory cytokines and markers of an alternatively activated macrophage response. IFN-γ can increase IgE+Ag-dependent production of IL-6 and IL-13 by mast cells in vitro through effects mediated by IFN-γR (Figure 2). Consistent with these findings, OVA treatment significantly enhanced lung expression of IL-6 and IL-13 in WT or WT BMCMCs→$Kit^{W-sh/W-sh}$ mice but not in mast cell–deficient $Kit^{W-sh/W-sh}$ mice or in $Kit^{W-sh/W-sh}$ mice containing mast cells that lacked either IFN-γR or FcεRIγ (Figure 7, A and B). Our microarray-based

screen for increased gene expression identified both IL-33 and markers of an alternatively activated macrophage response as substantially upregulated in this model in OVA-sensitized and challenged WT mice. IL-33 is a member of the IL-1 family that is produced mainly by fibroblasts, epithelial cells, and endothelial cells (44). The receptor for IL-33 is composed of two units, the orphan receptor ST2 and IL-1 receptor accessory protein (IL-1RACP) (44). IL-33 can amplify both Th1 and Th2 responses (44) and can directly induce cytokine production by mast cells (including IL-13 production; ref. 45) or basophils, as well as enhance IgE+Ag-dependent activation of these cells (44–46). In the presence of IL-13, IL-33 also can promote polarization of alveolar macrophages toward an alternatively activated macrophage phenotype in vitro or in vivo (47). OVA sensitization and challenge markedly increased lung levels of IL-33 in a manner that was largely, but not entirely, mast cell dependent, and the mast cell–dependent component of this response required that mast cells express both IFN-γR and FcεRIγ (Figure 7C).

Th2 responses, including those associated with models of airway allergic inflammation, are often associated with the development of an alternatively activated macrophage response (48). Such responses, which contribute to the mitigation or resolution of the pathology associated with allergic inflammation (48), can include increased lung expression of the macrophage receptor with collage-
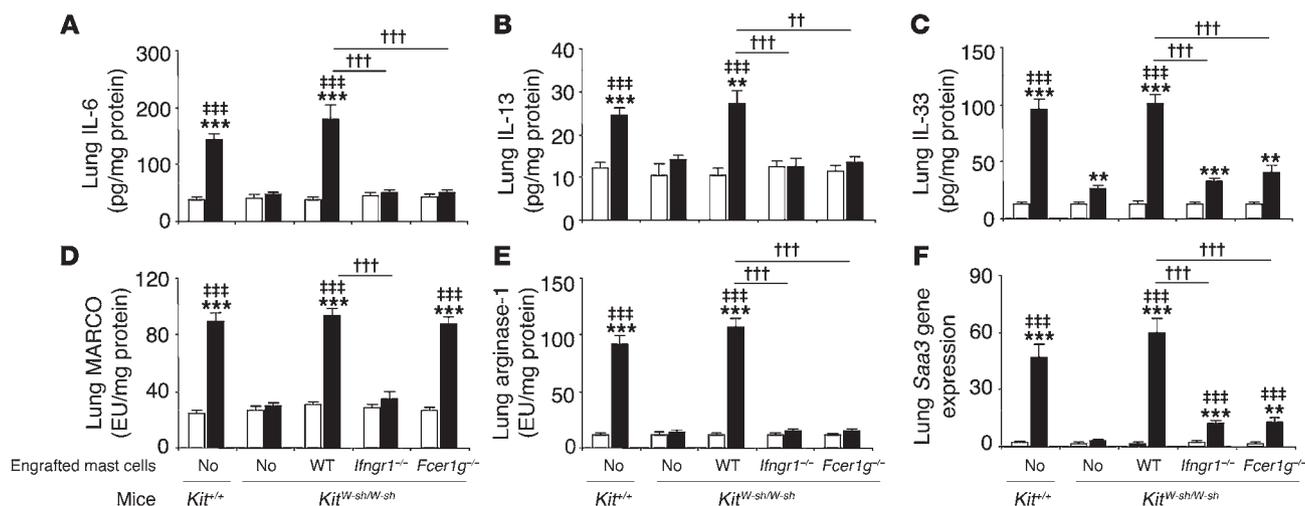
Figure 7
Levels of inflammatory cytokines and other molecules in the lung. Levels of IL-6 (**A**), IL-13 (**B**), IL-33 (**C**), MARCO (**D**), and arginase-1 protein (**E**) and the relative levels of *Saa3* mRNA (**F**) were measured in the lungs 24 hours after the ninth OVA or PBS challenge in WT C57BL/6 (*Kit*$^{+/+}$), mast cell–deficient C57BL/6-*Kit*$^{W-sh/W-sh}$ (*Kit*$^{W-sh/W-sh}$), C57BL/6 (WT) BMCMCs→ C57BL/6-*Kit*$^{W-sh/W-sh}$, *Ifngr1*$^{-/-}$ BMCMCs→ C57BL/6-*Kit*$^{W-sh/W-sh}$, and *Fcer1g*$^{-/-}$ BMCMCs→ C57BL/6-*Kit*$^{W-sh/W-sh}$ mice and the corresponding PBS-treated control mice. White bars: PBS-treated groups; black bars: OVA-sensitized and -challenged groups. **$P < 0.01$, ***$P < 0.001$ versus the corresponding PBS controls; ‡‡‡$P < 0.001$ versus OVA-sensitized and -challenged *Kit*$^{W-sh/W-sh}$ mice; ††$P < 0.01$, †††$P < 0.001$ versus group indicated. $n = 6$–10 per group. EU, experimental units, with the arbitrary value of 100 EU assigned to the values for the MARCO (**D**) or arginase-1 (**E**) content in the lung protein extract of 4 randomly selected WT C57BL/6 mice in the OVA-sensitized and -challenged group.

nous structure (MARCO) (49) (thought be involved in host defense against modified lipids and tissue repair [ref. 50] and in regulating the tissue distribution and differentiation of macrophages [ref. 51]); the enzyme arginase-1 (48) (which can be increased in allergen-induced lung inflammation, but whose role in the pathogenesis of asthma is unresolved; refs. 52, 53); and the acute-phase protein serum amyloid A3 (SAA3) (54) (which is elevated in a mouse model of allergic inflammation [ref. 55] and may contribute to the accumulation of myeloid cells and to enhancing expression of chemoattractants in this setting [ref. 56]). We found that antigen sensitization and challenge resulted in mast cell–dependent increases in lung levels of each of these proteins (Figure 7, D–F). Mast cell responsiveness to IFN-γ, but not mast cell expression of FcεRIγ, was required to effect mast cell–dependent increases in MARCO in antigen-challenged mice (Figure 7D). By contrast, mast cell signaling via both IFN-γR and FcεRIγ was required to effect the striking antigen- and mast cell–dependent increases in lung levels of arginase-1 protein and *Saa3* mRNA (Figure 7, E and F).

Discussion

Our findings reveal an important and previously unsuspected role for IFN-γ–dependent activation of mast cells in the development of the inflammation and tissue pathology associated with this mouse model of chronic allergic inflammation of the airways. As summarized in Supplemental Table 1, mast cell expression of IFN-γR is required for optimal development of many features of this model, including AHR to methacholine, inflammation of the airways (with infiltrates containing many neutrophils and eosinophils), airway remodeling (i.e., increases in both numbers of epithelial goblet cells and lung collagen), and markedly increased lung expression of several cytokines, chemokines, and markers of an alternatively activated macrophage response. It bears emphasis that in *Kit*$^{W-sh/W-sh}$ mice

engrafted with *Ifngr1*$^{-/-}$ mast cells, mast cells are the only cells that genetically lack IFN-γR. The poor development of many important features of this model in such mice therefore demonstrates that these features require functions of IFN-γ–responsive mast cells that cannot be provided adequately by any of the other IFN-γ–responsive cell types present in this setting.

Mast cell expression of IFN-γR is required for optimal expression of most of the effects of mast cells in this model that also require mast cell expression of FcεRIγ (Supplemental Table 1), and this model is associated with significant, but mast cell–independent, elevations of levels of IFN-γ in the affected lungs (Figure 3A). In vitro, costimulation of mouse mast cells with IFN-γ significantly enhanced their ability to release histamine, IL-6, and IL-13 in response to activation with IgE and specific antigen (Figure 2), and IFN-γ dose-dependently enhanced the IgE+Ag-dependent release of IL-6 and IL-13 by mast cells in concentrations as low as 0.1 ng/ml (Supplemental Figure 2). In vivo, the significant increases in lung levels of IL-6, IL-13, and IL-33 in this model occurred by wholly (for IL-6 and IL-13) or largely (for IL-33) mast cell–dependent mechanisms (Figure 7, A–C). Moreover, such mast cell–dependent elevations in lung levels of these cytokines required that mast cells express both FcεRIγ and IFN-γR1 (Figure 7, A–C). Taken together, these findings are consistent with the hypothesis that elevations of lung levels of IFN-γ are mechanistically upstream of mast cells in this model and that costimulation of mast cells with IFN-γ (via IFN-γR) and via FcεRIγ results in increased production of IL-6, IL-13, and IL-33, by mast cells (especially for IL-6 and IL-13) and/or other cells that produce these cytokines in a mast cell–dependent manner.

Most of the other features of the model that we analyzed — including striking mast cell–dependent increases in airway responses to antigen or airway hyperreactivity to methacholine (Figure 4), tissue neutrophils and eosinophils (Figure 5, K and L,

respectively) and BAL fluid leukocytes (Figure 5), and lung levels of a panel of chemokines (Supplemental Figure 6) — were affected equally (and, in general, markedly diminished) by a lack of either mast cell IFN-γR or mast cell FcεRIγ (Supplemental Table 1). These results indicate that signaling via both IFN-γR and FcεRIγ is required for mast cells to perform the functions important for the development of these mast cell–dependent features of the model. However, some of the in vivo effects of mast cell activation via IFN-γR or FcεRIγ are distinct. The increase in lung mast cells in this model is critically dependent on mast cell FcεRIγ, as revealed both in this (Figure 5M) and in our prior study (29), but this expansion of lung mast cells occurs independently of mast cell IFN-γR (Figure 5M). Because mast cells that lack FcεRIγ exhibit ablation of signaling through FcεRIγ and, as a consequence of that, are significantly impaired in their ability to expand in numbers in the lungs in this model of chronic allergic inflammation, changes in the pathology that are affected by the lack of mast cell expression of FcεRIγ might reflect the lack of FcεRIγ-dependent signaling in those mast cells that are present in such animals, the reduced numbers of lung mast cells in these mice, or both.

Regarding features of lung remodeling, mast cells lacking either IFN-γR or FcεRIγ were equally and markedly impaired in their ability to increase levels of lung collagen (Figure 6F) and TIMP-1 protein (Figure 6H). However, the marked mast cell–dependent increase in lung levels of integrin α7 protein in this model was completely ablated if mast cells lacked IFN-γR but only modestly, albeit significantly, reduced if mast cells lacked FcεRIγ (Figure 6I). Similarly, the marked and apparently entirely mast cell–dependent increase in lung levels of MARCO protein in this model required that mast cells express IFN-γR but not FcεRIγ (Figure 7D). By contrast, two other markers of an alternatively activated macrophage response, substantially increased lung levels of arginase-1 protein and *Saa3* mRNA, were also induced in a largely or entirely mast cell–dependent manner, but in this case the effect was either ablated (in the case of arginase-1 protein; Figure 7E) or markedly reduced (in the case of *Saa3* mRNA; Figure 7F) if mast cells lacked either IFN-γR or FcεRIγ. Finally, our data indicate that one important feature of the model, the development of large numbers of intraepithelial goblet cells, is entirely mast cell dependent but that this function can be largely sustained by mast cells lacking either IFN-γR or FcεRIγ (Figure 6G).

Our results support the conclusion that optimal expression of many critical mast cell functions in this model requires costimulation of the cells via both IFN-γ/IFN-γR and FcεRIγ, whereas other mast cell functions can be influenced by each receptor independently of the other. We do not know why costimulation of mast cells with IFN-γ is important for the development of so many, but not all, of the features of this model of chronic allergic inflammation. Nor can our mast cell engraftment approach permit one to determine whether particular "mast cell–dependent" features of the model reflect direct actions of mast cells (such as effects of mast cell–derived mediators on leukocytes or structural cells) or indirect effects (such as those mediated by other cells of innate or acquired immunity that are recruited to, and/or influenced in, the lungs in a mast cell–dependent manner). However, our study clearly establishes that mast cell responsiveness to IFN-γ, a cytokine classically regarded as a marker of a Th1 response, is as critical for the development of many features of the inflammation, tissue remodeling, and airway functional changes observed in this model of chronic allergic inflammation of the airways as is mast cell expression of FcεRIγ. Moreover, our in vitro findings show that even low concentrations of IFN-γ can enhance

IgE+Ag-dependent release of cytokines by mast cells (Figure 2 and Supplemental Figure 2), suggesting that this mechanism may influence IgE-dependent mast cell functions in many settings, not just those associated with marked elevations of IFN-γ.

Others have shown that various populations of rodent and human mast cells can express IFN-γR or respond to IFN-γ in vitro (31–34), but the importance of mast cell expression of IFN-γR in vivo was not clear. The unexpected identification of an IFN-γ/mast cell axis in this mouse model of airway allergic inflammation challenges the notion that the mast cell's function in this and perhaps other models of chronic allergic inflammation is entirely or predominantly under the control of the Th2 cell response. Moreover, treatment with a single injection of a neutralizing antibody to IFN-γ, administered to mice 3 hours after the last OVA challenge, reduced the magnitude of both the Penh response and the increases in BAL fluid leukocytes induced by antigen challenge (Supplemental Figure 1), findings indicating that IFN-γ represents a therapeutic target in this mouse model.

Are these findings relevant to human asthma? One always must be cautious in attempting to extrapolate findings from any animal model of a disease to its human counterpart, and the relevance of our observations in mice to asthma in humans remains to be determined. For example, while it is well established that the phenotypic features of mast cells can vary based on species, anatomical site, and exposure to cytokines and other factors in the cells' microenvironments (57, 58), little is known about the regulation of the surface expression of IFN-γR by mast cells, whether in the airways or in any other site. Moreover, the relationship of our mouse model of chronic allergic inflammation of the airways to particular clinical subtypes of human asthma is not clear. However, as a first step toward addressing the relationship of our mouse model to human asthma, we used gene set enrichment analysis (GSEA) (59) to compare the set of genes that Laprise et al. (60) reported were upregulated in the bronchial biopsy specimens from 4 allergic asthmatic subjects with mild asthma (compared with those from 4 control subjects without asthma) and those genes that were upregulated in our mouse model in OVA-sensitized and -challenged (vs. PBS-treated control) mice. We detected significant (i.e., $P < 0.05$) similarity between genes upregulated in the human asthma specimens compared with those upregulated in our model in WT mice ($P \sim 0.021$) or WT mast cell–engrafted $Kit^{W-sh/W-sh}$ mice ($P \sim 0.020$), but not in identically sensitized and challenged mast cell–deficient $Kit^{W-sh/W-sh}$ mice or in $Kit^{W-sh/W-sh}$ mice engrafted with $Ifngr1^{-/-}$ or $Fcer1g^{-/-}$ mast cells (Supplemental Figures 7–12 and Supplemental Tables 2 and 3). While these findings are intriguing, it will be of interest to repeat such GSEA studies using data sets derived from additional subsets of asthma subjects, including those with increased numbers of airway neutrophils and/or increased levels of IFN-γ in the lung, when data of this type become available. Such work, together with other studies in human subjects, will be important in the attempt to decide whether IFN-γ merits investigation as a therapeutic target for reducing the pathology characteristic of IgE-associated allergic inflammation in asthma and perhaps other settings.

Methods

Mice. C57BL/6 WT, *Ifng*$^{-/-}$, and *Ifngr1*$^{-/-}$ mice were originally purchased from The Jackson Laboratory. C57BL/6-*Kit*$^{W-sh/W-sh}$ mice were provided by Peter Besmer (Molecular Biology Program, Memorial Sloan-Kettering Cancer Center, New York, New York, USA); these mice were then backcrossed to C57BL/6J for more than 10 generations. All of the C57BL/6 WT mice and C57BL/6-

$Kit^{W-sh/W-sh}$ mice used in the experiments reported herein were bred and raised in the same room in the Stanford Laboratory Animal Facility. $Fcer1g^{-/-}$ mice on the C57BL/6 background (B6.129P2-Fcεr1gtm1Rav N12) were purchased from Taconic. Age-matched female mice were used for all experiments. All animal care and experimentation reported herein were conducted in compliance with the guidelines of the NIH and with the specific approval of the Institutional Animal Care and Use Committee of Stanford University.

Mast cell engraftment. Engraftment of mast cells in mast cell–deficient C57BL/6-$Kit^{W-sh/W-sh}$ mice was performed as described previously (29), with minor modifications. Bone marrow cells derived from 4-week-old female C57BL/6, C57BL/6-$Ifngr1^{-/-}$, or C57BL/6-$Fcer1g^{-/-}$ mice were cultured in WEHI-3–conditioned medium (ATCC TIB-68), as a source of IL-3, for 4–5 weeks to generate cell populations that contained more than 99% immature mast cells (BMCMCs). BMCMCs (5×10^6) were injected into each mouse via the tail vein, and the recipients (e.g., WT BMCMCs→$Kit^{W-sh/W-sh}$, $Ifngr1^{-/-}$ BMCMCs→$Kit^{W-sh/W-sh}$, or $Fcer1g^{-/-}$ BMCMCs→$Kit^{W-sh/W-sh}$ mice) were used for experiments 18 weeks later.

Production of histamine, cytokines, and chemokines by mast cells in vitro. BMCMCs were derived as described above and in ref. 29 from femoral bone marrow cells of C57BL/6 WT, $Ifngr1^{-/-}$, and $Fcer1g^{-/-}$ mice and were sensitized with 1 μg/ml H1-ε26 anti-DNP IgE at 37°C overnight. After IgE sensitization, BMCMCs were suspended in DMEM medium (MediaTech) supplemented with 10% heat-inactivated FCS (Sigma-Aldrich), 50 μM 2-ME (Sigma-Aldrich), 50 μg/ml streptomycin (Invitrogen), and 50 U/ml penicillin (Invitrogen) at a final concentration of 5×10^5 cells/ml. For activation of the BMCMCs, antigen (DNP-HSA; Sigma-Aldrich) was added to the culture medium at various final concentrations (e.g., 1, 10, or 20 ng/ml). In some groups, we also added rmIFN-γ (PeproTech) at a final concentration of 0.1 to 100 ng/ml. One hour (for calculation of % histamine release) or 24 hours (for measurements of secreted cytokines) after cell activation with antigen with or without rmIFN-γ, BMCMC culture supernatants were collected and stored at –80°C and then were used for measurements of histamine, cytokines, and chemokines.

Immunization and airway challenge with antigen. Mice were immunized by 3 i.p. injections of 50 μg OVA (Sigma-Aldrich) in 0.1 ml PBS on days 1, 4, and 7 (29). Starting on day 12, mice were challenged i.n. with 20 μg OVA in 30 μl PBS weekly for 9 weeks; control mice received i.p. injections and i.n. challenges with PBS on the same schedule (29).

Measurement of airway reactivity to methacholine. Twenty-four hours after the eighth OVA or PBS challenge, responses to aerosolized methacholine were measured using whole-body plethysmography (Buxco Systems). Responses to antigen (OVA) or PBS were assessed by recording Penh over 10-minute time periods at intervals before and after the ninth (final) OVA or PBS challenge (in the absence of methacholine). We also performed invasive measurements of airway reactivity in anesthetized, tracheostomized, mechanically ventilated mice. Aerosolized methacholine was administered in increasing concentrations (0, 1.25, 2.5, 5, and 10 mg/ml), with individual doses separated by 2 minutes. R_L and C_{dyn} were continuously computed by fitting flow, volume, and pressure to an equation of motion for each aerosol challenge period, which consisted of a 0.5-minute aerosol exposure and a 1.5-minute period after exposure.

BAL and histology. For BAL, mice were killed by CO_2 inhalation 24 hours after the last (ninth) OVA or PBS challenge. The left lung was ligated and removed for measurements of proteins or mRNA (see below), whereas the right lung lobes were lavaged once with ice-cold HBSS (BAL), then fixed (10% formaldehyde) and paraffin-embedded. Paraffin sections of 5 μm were mounted on Superfrost Plus glass slides (Fisher Scientific) and stained with H&E, toluidine blue, or Masson trichrome stains. Numbers of peribronchial neutrophils, eosinophils, and mast cells were determined using the method described by Pope et al. (61).

Gene expression measurements. Three or 4 mice were randomly selected from each of the 5 different groups of PBS-treated or OVA-sensitized and challenged mice, and specimens of their homogenized left lungs were subjected to total RNA isolation using TRIzol Reagent (Invitrogen). Microarray hybridization was performed using the individually isolated RNA samples at the Stanford Protein and Nucleic Acid facility with Affymetrix Mouse Genome 430 2.0 arrays (Affymetrix). The array data were processed using GCRMA (62) and entered into the Gene Expression Omnibus with the accession number GSE27066. A set of 96 upregulated genes in human asthma were identified by quantile normalization and Significance Analysis of Microarrays (63) of a publicly available gene expression data set (60), and the enrichment of the 67 genes in this set with homologs measured on the mice arrays was evaluated using GSEA (see Supplemental Methods for additional information about methods used for GSEA) (59).

Extraction of lung tissue protein. Lung tissue protein was extracted using the T-PER Tissue Protein Extraction Reagent purchased from Thermo Scientific. Half of the left lung was placed into 1 ml of protein extraction reagent, followed by homogenization, then the samples were centrifuged at 10,000 g for 5 minutes to pellet cell/tissue debris; the supernatants were collected for further analyses.

ELISA measurements of plasma antibodies. Plasma was collected 24 hours after the ninth OVA or PBS challenge. ELISA kits for total plasma IgE and IgG_1 were purchased from Bethyl Laboratories; the ELISA kit for OVA-specific IgE was purchased from MD Biosciences. Concentrations of OVA-specific IgG_1 in the plasma were measured by direct ELISA (29).

Measurements of histamine, cytokines, chemokines, and other molecules. Histamine in the BMCMC culture supernatants was measured using an Enzyme Immunoassay Kit (Beckman Coulter) according to the manufacturer's instructions, and the results were expressed as percent histamine release (64). ELISA kits for CXCL1, CXCL2, CCL9, CCL11, CCL12, CCL24, IL-33, and TIMP-1 were purchased from R&D Systems; ELISA kits for IL-4, IL-6, IL-17, IL-13, and IFN-γ were purchased from eBioscience. We used direct ELISA methods to measure levels of MARCO, integrin α7, and arginase-1. Primary antibodies against MARCO or integrin α7 were purchased form R&D Systems, and primary antibodies against arginase-1 were purchased form Novus Biologicals.

Measurement of protein and collagen. The protein levels of tissue samples were measured using a BCA Protein Assay Kit form Thermo Scientific. Tissue collagen levels were measured using a Sircol Soluble Collagen Assay Kit from Biocolor Life Science Assays.

Quantitative RT-PCR. Total RNA isolated from the left lungs using TRIzol Reagent (Invitrogen) was reverse transcribed using the High-Capacity cDNA Archive Kit (Applied Biosystems) according to the manufacturer's instructions. Quantitative real-time PCR was performed using the ABI 7500 Real-Time PCR System (Applied Biosystems) with the following cycling parameters: 10 minutes at 95°C, then 40 biphasic cycles of 15 seconds at 95°C, and 1 minute at 60°C. Primers and probes for SAA3 were purchased from Applied Biosystems.

Statistics. Unless otherwise specified, differences in airway response between groups were tested for statistical significance using ANOVA. The unpaired Student's *t* test (2 tailed) was used for all other analyses. A P value less than 0.05 was considered statistically significant. Unless otherwise specified, all data are presented as mean ± SEM or mean + SEM.

research article

Address correspondence to: Stephen J. Galli, Department of Pathology, L-235, Stanford University School of Medicine, 300 Pasteur Drive, Stanford, California 94305-5324, USA. Phone: 650.723.7975; Fax: 650.725.6902; E-mail: sgalli@stanford.edu. Or to: Mang Yu, Department of Pathology, Center for Clinical Sciences Research, 269 Campus Dr. #3255, Stanford, California 94305-5176, USA. Phone: 650.736.0069; Fax: 650.736.0073; E-mail: yumyu@stanford.edu.

1. Busse WW, Lemanske RF Jr. Asthma. *N Engl J Med.* 2001;344(5):350–362.
2. Umetsu DT, McIntire JJ, Akbari O, Macaubas C, DeKruyff RH. Asthma: an epidemic of dysregulated immunity. *Nat Immunol.* 2002;3(8):715–720.
3. Wills-Karp M. Immunologic basis of antigen-induced airway hyperresponsiveness. *Annu Rev Immunol.* 1999;17:255–281.
4. Holgate ST. Novel targets of therapy in asthma. *Curr Opin Pulm Med.* 2009;15(1):63–71.
5. Fahy JV. Eosinophilic and neutrophilic inflammation in asthma: insights from clinical studies. *Proc Am Thorac Soc.* 2009;6(3):256–259.
6. Wenzel SE, Szefler SJ, Leung DY, Sloan SI, Rex MD, Martin RJ. Bronchoscopic evaluation of severe asthma. Persistent inflammation associated with high dose glucocorticoids. *Am J Respir Crit Care Med.* 1997;156(3 pt 1):737–743.
7. Gibson PG, Simpson JL, Saltos N. Heterogeneity of airway inflammation in persistent asthma: evidence of neutrophilic inflammation and increased sputum interleukin-8. *Chest.* 2001;119(5):1329–1336.
8. Sur S, et al. Sudden-onset fatal asthma. A distinct entity with few eosinophils and relatively more neutrophils in the airway submucosa? *Am Rev Respir Dis.* 1993;148(3):713–719.
9. Jatakanon A, Uasuf C, Maziak W, Lim S, Chung KF, Barnes PJ. Neutrophilic inflammation in severe persistent asthma. *Am J Respir Crit Care Med.* 1999;160(5 pt 1):1532–1539.
10. Woodruff PG, et al. Relationship between airway inflammation, hyperresponsiveness, and obstruction in asthma. *J Allergy Clin Immunol.* 2001;108(5):753–758.
11. Shaw DE, et al. Association between neutrophilic airway inflammation and airflow limitation in adults with asthma. *Chest.* 2007;132(6):1871–1875.
12. Wenzel SE, et al. Evidence that severe asthma can be divided pathologically into two inflammatory subtypes with distinct physiologic and clinical characteristics. *Am J Respir Crit Care Med.* 1999;160(3):1001–1008.
13. [No authors listed]. The ENFUMOSA cross-sectional European multicentre study of the clinical phenotype of chronic severe asthma. European Network for Understanding Mechanisms of Severe Asthma. *Eur Respir J.* 2003;22(3):470–477.
14. Cembrzynska-Nowak M, Szklarz E, Inglot AD, Teodorczyk-Injeyan JA. Elevated release of tumor necrosis factor-α and interferon-γ by bronchoalveolar leukocytes from patients with bronchial asthma. *Am Rev Respir Dis.* 1993;147(2):291–295.
15. Shannon J, et al. Differences in airway cytokine profile in severe asthma compared to moderate asthma. *Chest.* 2008;133(2):420–426.
16. McMillan SJ, Lloyd CM. Prolonged allergen challenge in mice leads to persistent airway remodelling. *Clin Exp Allergy.* 2004;34(3):497–507.
17. Hansen G, Berry G, DeKruyff RH, Umetsu DT. Allergen-specific Th1 cells fail to counterbalance Th2 cell-induced airway hyperreactivity but cause severe airway inflammation. *J Clin Invest.* 1999;103(2):175–183.
18. Cohn L, Homer RJ, Niu N, Bottomly K. T helper 1 cells and interferon γ regulate allergic airway inflammation and mucus production. *J Exp Med.* 1999;190(9):1309–1318.

19. Huang TJ, et al. Allergen-specific Th1 cells counteract efferent Th2 cell-dependent bronchial hyperresponsiveness and eosinophilic inflammation partly via IFN-γ. *J Immunol.* 2001;166(1):207–217.
20. Yoshida M, et al. Effect of interferon-γ on allergic airway responses in interferon-γ-deficient mice. *Am J Respir Crit Care Med.* 2002;166(4):451–456.
21. Koch M, et al. Role of local pulmonary IFN-γ expression in murine allergic airway inflammation. *Am J Respir Cell Mol Biol.* 2006;35(2):211–219.
22. Coyle AJ, et al. Mice lacking the IFN-γ receptor have impaired ability to resolve a lung eosinophilic inflammatory response associated with a prolonged capacity of T cells to exhibit a Th2 cytokine profile. *J Immunol.* 1996;156(8):2680–2685.
23. Randolph DA, Stephens R, Carruthers CJ, Chaplin DD. Cooperation between Th1 and Th2 cells in a murine model of eosinophilic airway inflammation. *J Clin Invest.* 1999;104(8):1021–1029.
24. Fulkerson PC, Zimmermann N, Hassman LM, Finkelman FD, Rothenberg ME. Pulmonary chemokine expression is coordinately regulated by STAT1, STAT6, and IFN-γ. *J Immunol.* 2004;173(12):7565–7574.
25. Boehm U, Klamp T, Groot M, Howard JC. Cellular responses to interferon-γ. *Annu Rev Immunol.* 1997;15:749–795.
26. Frucht DM, Fukao T, Bogdan C, Schindler H, O'Shea JJ, Koyasu S. IFN-γ production by antigen-presenting cells: mechanisms emerge. *Trends Immunol.* 2001;22(10):556–560.
27. Szabo SJ, Sullivan BM, Peng SL, Glimcher LH. Molecular mechanisms regulating Th1 immune responses. *Annu Rev Immunol.* 2003;21:713–758.
28. Tau G, Rothman P. Biologic functions of the IFN-γ receptors. *Allergy.* 1999;54(12):1233–1251.
29. Yu M, Tsai M, Tam SY, Jones C, Zehnder J, Galli SJ. Mast cells can promote the development of multiple features of chronic asthma in mice. *J Clin Invest.* 2006;116(6):1633–1641.
30. Carlow DA, Teh SJ, Teh HS. Specific antiviral activity demonstrated by TGTP, a member of a new family of interferon-induced GTPases. *J Immunol.* 1998;161(5):2348–2355.
31. Nafziger J, Arock M, Guillosson JJ, Wietzerbin J. Specific high-affinity receptors for interferon-γ on mouse bone marrow-derived mast cells: inhibitory effect of interferon-γ on mast cell precursors. *Eur J Immunol.* 1990;20(1):113–117.
32. Yanagida M, et al. Interferon-γ promotes the survival and FcεRI-mediated histamine release in cultured human mast cells. *Immunology.* 1996;89(4):547–552.
33. Holliday MR, Banks EM, Dearman RJ, Kimber I, Coleman JW. Interactions of IFN-γ with IL-3 and IL-4 in the regulation of serotonin and arachidonate release from mouse peritoneal mast cells. *Immunology.* 1994;82(1):70–74.
34. Bissonnette EY, Chin B, Befus AD. Interferons differentially regulate histamine and TNF-α in rat intestinal mucosal mast cells. *Immunology.* 1995;86(1):12–17.
35. Lewis CC, et al. Unique and overlapping gene expression patterns driven by IL-4 and IL-13 in the mouse lung. *J Allergy Clin Immunol.* 2009;123(4):795–804.
36. Finkelman FD, Hogan SP, Hershey GK, Rothenberg ME, Wills-Karp M. Importance of cytokines in murine allergic airway disease and human asthma. *J Immunol.* 2010;184(4):1663–1674.

37. Williams CM, Galli SJ. Mast cells can amplify airway reactivity and features of chronic inflammation in an asthma model in mice. *J Exp Med.* 2000;192(3):455–462.
38. Wolters PJ, et al. Tissue-selective mast cell reconstitution and differential lung gene expression in mast cell-deficient *Kit^{W-sh}/Kit^{W-sh}* sash mice. *Clin Exp Allergy.* 2005;35(1):82–88.
39. Grimbaldeston MA, Chen CC, Piliponsky AM, Tsai M, Tam SY, Galli SJ. Mast cell-deficient *W-sash* c-kit mutant *Kit^{W-sh/W-sh}* mice as a model for investigating mast cell biology in vivo. *Am J Pathol.* 2005;167(3):835–848.
40. Matsumoto H, et al. Relationship of airway wall thickening to an imbalance between matrix metalloproteinase-9 and its inhibitor in asthma. *Thorax.* 2005;60(4):277–281.
41. Liu J, Burkin DJ, Kaufman SJ. Increasing α7β1-integrin promotes muscle cell proliferation, adhesion, and resistance to apoptosis without changing gene expression. *Am J Physiol Cell Physiol.* 2008;294(2):C627–C640.
42. Tran T, et al. Laminin-binding integrin α7 is required for contractile phenotype expression by human airway myocytes. *Am J Respir Cell Mol Biol.* 2007;37(6):668–680.
43. Chin AC, Parkos CA. Pathobiology of neutrophil transepithelial migration: implications in mediating epithelial injury. *Annu Rev Pathol.* 2007;2:111–143.
44. Liew FY, Pitman NI, McInnes IB. Disease-associated functions of IL-33: the new kid in the IL-1 family. *Nat Rev Immunol.* 2010;10(2):103–110.
45. Ho LH, et al. IL-33 induces IL-13 production by mouse mast cells independently of IgE-FcεRI signals. *J Leukoc Biol.* 2007;82(6):1481–1490.
46. Silver MR, Margulis A, Wood N, Goldman SJ, Kasaian M, Chaudhary D. IL-33 synergizes with IgE-dependent and IgE-independent agents to promote mast cell and basophil activation. *Inflamm Res.* 2010;59(3):207–218.
47. Kurowska-Stolarska M, et al. IL-33 amplifies the polarization of alternatively activated macrophages that contribute to airway inflammation. *J Immunol.* 2009;183(10):6469–6477.
48. Martinez FO, Helming L, Gordon S. Alternative activation of macrophages: an immunologic functional perspective. *Annu Rev Immunol.* 2009;27:451–483.
49. Bowdish DM, Gordon S. Conserved domains of the class A scavenger receptors: evolution and function. *Immunol Rev.* 2009;227(1):19–31.
50. Dahl M, et al. Protection against inhaled oxidants through scavenging of oxidized lipids by macrophage receptors MARCO and SR-AI/II. *J Clin Invest.* 2007;117(3):757–764.
51. Chen Y, et al. Defective microarchitecture of the spleen marginal zone and impaired response to a thymus-independent type 2 antigen in mice lacking scavenger receptors MARCO and SR-A. *J Immunol.* 2005;175(12):8173–8180.
52. North ML, Khanna N, Marsden PA, Grasemann H, Scott JA. Functionally important role for arginase 1 in the airway hyperresponsiveness of asthma. *Am J Physiol Lung Cell Mol Physiol.* 2009;296(6):L911–L920.
53. Niese KA, et al. Bone marrow cell derived arginase I is the major source of allergen-induced lung arginase but is not required for airway hyperresponsiveness, remodeling and lung inflammatory responses

in mice. *BMC Immunol*. 2009;10:33.

54. Meek RL, Eriksen N, Benditt EP. Murine serum amyloid A3 is a high density apolipoprotein and is secreted by macrophages. *Proc Natl Acad Sci U S A*. 1992;89(17):7949–7952.

55. Jaradat M, et al. Modulatory role for retinoid-related orphan receptor alpha in allergen-induced lung inflammation. *Am J Respir Crit Care Med*. 2006; 174(12):1299–1309.

56. Hiratsuka S, et al. The S100A8-serum amyloid A3-TLR4 paracrine cascade establishes a pre-metastatic phase. *Nat Cell Biol*. 2008;10(11):1349–1355.

57. Metcalfe DD, Baram D, Mekori YA. Mast cells. *Physiol Rev*. 1997;77(4):1033–1079.

58. Galli SJ, Kalesnikoff J, Grimbaldeston MA, Piliponsky AM, Williams CM, Tsai M. Mast cells as "tunable" effector and immunoregulatory cells: recent advances. *Annu Rev Immunol*. 2005;23:749–786.

59. Subramanian A, et al. Gene set enrichment analysis: a knowledge-based approach for interpreting genome-wide expression profiles. *Proc Natl Acad Sci U S A*. 2005;102(43):15545–15550.

60. Laprise C, Sladek R, Ponton A, Bernier MC, Hudson TJ, Laviolette M. Functional classes of bronchial mucosa genes that are differentially expressed in asthma. *BMC Genomics*. 2004;5(1):21.

61. Pope SM, Zimmermann N, Stringer KF, Karow ML, Rothenberg ME. The eotaxin chemokines and CCR3 are fundamental regulators of allergen-induced pulmonary eosinophilia. *J Immunol*. 2005;175(8):5341–5350.

62. Gentleman RC, et al. Bioconductor: open software development for computational biology and bioinformatics. *Genome Biol*. 2004;5(10):R80.

63. Tusher VG, Tibshirani R, Chu G. Significance analysis of microarrays applied to the ionizing radiation response. *Proc Natl Acad Sci U S A*. 2001; 98(9):5116–5121.

64. Barrett KE, Pluznik DH, Metcalfe DD. Histamine release from the cultured mouse mast cell line PT18 in response to immunologic and non–immunologic stimuli. *Agents Actions*. 1984;14(3–4):488–493.